



THE UNIVERSITY *of* EDINBURGH

Edinburgh Research Explorer

MicroRNA-34a Acutely Regulates Synaptic Efficacy in the Adult Dentate Gyrus In Vivo

Citation for published version:

Berentsen, B, Patil, S, Rønnestad, K, Goff, KM, Pajak, M, Simpson, TI, Wibrand, K & Bramham, CR 2020, 'MicroRNA-34a Acutely Regulates Synaptic Efficacy in the Adult Dentate Gyrus In Vivo', *Molecular Neurobiology*, vol. 57, no. 3, pp. 1432–1445. <https://doi.org/10.1007/s12035-019-01816-1>

Digital Object Identifier (DOI):

[10.1007/s12035-019-01816-1](https://doi.org/10.1007/s12035-019-01816-1)

Link:

[Link to publication record in Edinburgh Research Explorer](#)

Document Version:

Version created as part of publication process; publisher's layout; not normally made publicly available

Published In:

Molecular Neurobiology

General rights

Copyright for the publications made accessible via the Edinburgh Research Explorer is retained by the author(s) and / or other copyright owners and it is a condition of accessing these publications that users recognise and abide by the legal requirements associated with these rights.

Take down policy

The University of Edinburgh has made every reasonable effort to ensure that Edinburgh Research Explorer content complies with UK legislation. If you believe that the public display of this file breaches copyright please contact openaccess@ed.ac.uk providing details, and we will remove access to the work immediately and investigate your claim.



MicroRNA-34a Acutely Regulates Synaptic Efficacy in the Adult Dentate Gyrus In Vivo

B. Berentsen^{1,2} · S. Patil^{1,2} · K. Rønnestad^{1,2} · K. M. Goff^{1,2} · M. Pajak³ · T. I. Simpson³ · K. Wibrand^{1,2} · Clive R. Bramham^{1,2}

Received: 26 June 2019 / Accepted: 11 October 2019
© Springer Science+Business Media, LLC, part of Springer Nature 2019

Abstract

Activity-dependent synaptic plasticity involves rapid regulation of neuronal protein synthesis on a time-scale of minutes. miRNA function in synaptic plasticity and memory formation has been elucidated by stable experimental manipulation of miRNA expression and activity using transgenic approaches and viral vectors. However, the impact of rapid miRNA modulation on synaptic efficacy is unknown. Here, we examined the effect of acute (12 min), intrahippocampal infusion of a miR-34a antagonist (antimiR) on medial perforant path-evoked synaptic transmission in the dentate gyrus of adult anaesthetised rats. AntimiR-34a infusion acutely depressed medial perforant path-evoked field excitatory post-synaptic potentials (fEPSPs). The fEPSP decrease was detected within 9 min of infusion, lasted for hours, and was associated with knockdown of antimir-34a levels. Antimir-34a-induced synaptic depression was sequence-specific; no changes were elicited by infusion of scrambled or mismatch control. The rapid modulation suggests that a target, or set of targets, is regulated by miR-34a. Western blot analysis of dentate gyrus lysates revealed enhanced expression of Arc, a known miR-34a target, and four novel predicted targets (Ctip2, PKI-1 α , TCF4 and Ube2g1). Remarkably, antimiR-34a had no effect when infused during the maintenance phase of long-term potentiation. We conclude that miR-34a regulates basal synaptic efficacy in the adult dentate gyrus in vivo. To our knowledge, these in vivo findings are the first to demonstrate acute (< 9 min) regulation of synaptic efficacy in the adult brain by a miRNA.

Keywords microRNA · miR-34a · Gene expression · Hippocampus · Protein synthesis · Synaptic plasticity · Synaptic efficacy

Introduction

The highly pleiotropic nature of miRNAs has changed our view of neuronal development, function and aging. Some 60% of human genes may be post-transcriptionally regulated by miRNAs [1, 2], and in the brain, the list of miRNAs implicated in neuronal plasticity paradigms is growing [3, 4]. Synaptic stimulation resulting in long-term potentiation (LTP) and long-term depression (LTD) have been

demonstrated to involve tight temporal control of many brain-specific miRNAs, suggesting that miRNAs coordinate protein expression underlying the plasticity of synaptic transmission [3, 5–10]. Causal roles for specific miRNAs in LTP and LTD mechanisms have been identified using viral vectors to chronically knockdown microRNA expression or inhibit miRNA binding to target mRNA [11, 12]. Rapid, neuronal activity-dependent regulation of the RNA-induced silencing complex (RISC) has also been demonstrated [7, 13, 14]. However, to date, no miRNAs have been demonstrated to play an acute role in regulating synaptic strength on the order of minutes.

miR-34a plays a critical regulatory role in neurodegenerative diseases such as Alzheimer's disease (AD) [15], neuropsychiatric disorders such as bipolar disorder [16, 17], and schizophrenia [18], in addition to being implicated in development and many forms of cancer [19–21]. miR-34a has emerged as a key regulator of cell proliferation, apoptosis, and differentiation, and at least 77 targets that have been experimentally validated across multiple cell types [19]. miR-34a is ubiquitously expressed with the highest abundance in

Electronic supplementary material The online version of this article (<https://doi.org/10.1007/s12035-019-01816-1>) contains supplementary material, which is available to authorized users.

✉ Clive R. Bramham
clive.bramham@uib.no

¹ Department of Biomedicine, University of Bergen, Bergen, Norway

² KG Jebsen Centre for Neuropsychiatric Disorders, University of Bergen, Jonas Lies vei 91, 5009 Bergen, Norway

³ Institute for Adaptive and Neural Computation, School of Informatics, University of Edinburgh, Edinburgh, UK

the brain (and testes) [22]. In neurons, miR-34a has a somatodendritic distribution and it is implicated in the regulation of synaptic protein targets [23]. In the rat dentate gyrus in vivo, induction of LTP has been associated with enhanced miR-34a expression in the Argonaute 2/RISC [9] and altered total miR-34a expression in lysates samples [5, 8, 9]. Our previous work identified the immediate early gene Arc as a potential target of miR-34a. In cultured hippocampal neurons, overexpression of miR-34a resulted in downregulation of Arc expression [5]. Intriguingly, no changes in miR-34a were observed following brain-derived neurotrophic factor (BDNF) treatment in primary hippocampal neuronal cultures in vitro or following high-frequency stimulation (HFS)-induced LTP in vivo, despite increased Arc expression [5]. In total lysates, we have reported a small increase in miR-34a expression, and a large increase in Ago2-associated miR-34a expression, 30 min following LTP induction, in vivo [9]. The work suggested a preferential loading of miR-34a into the Ago2/RISC following HFS-induced NMDA-receptor-dependent LTP. In awake rats, miR-34a expression was shown to be reduced 20 min after LTP induction in the dentate gyrus, leading the authors to suggest that NMDA receptor-mediated reduction of miRNA levels out-competes an independent process working to increase miRNA expression [24].

Given the key role of Arc in activity-dependent synaptic plasticity and memory [25], we wanted to explore the possible role of endogenous miR-34a in regulating Arc expression and synaptic efficacy. Herein, we examined a possible role of endogenous miR-34a in the acute regulation of synaptic efficacy at medial perforant path (MPP)-dentate gyrus synapses in vivo. Using acute intrahippocampal infusion of miR-34a-targeting antimiR and corresponding mismatch and scrambled controls, we show that acute inhibition of miR-34a profoundly depresses MPP-evoked field EPSPs. Remarkably, antimiR-34a had no effect on synaptic transmission when infused during the maintenance phase of LTP. The results suggest that miR-34a plays a central role in regulating basal synaptic efficacy.

Materials and Methods

Reagents

Custom-made locked nucleic acid oligonucleotides antimiR-34a, mismatch antimiR-34a, and scrambled-antimiR-34a were obtained from Exiqon, Qiagen, (1 mM prepared in 1 × PBS). Sequences shown in Table S1. HiPerFect Transfection reagent 13.5% (Mat. No. 1029975; Lot No. 139311238; Qiagen) was diluted in PBS and added prior infusion to yield 1 mM and 100 μM concentrations. Custom-made 6-FAMTM Fluorescein antimiR-34a and scrambled-miR-34a (1 mM prepared in 1 × PBS; Exiqon) was used for evaluation of neuronal uptake,

distribution and localisation. Antibodies used for western blot analysis were Arc C7 mouse monoclonal (1:500, sc-17839), GAPDH mouse monoclonal (1:1000, sc-32233), PKI-1α goat polyclonal (1:1000, sc-1944), from Santa Cruz Biotech, USA and BCL11B/Ctip2 rabbit polyclonal (1:200, ABIN487046) Aviva Systems Biology, USA, TCF4; TCF7L2 rabbit polyclonal (1:1000, ABIN487067) Aviva Systems Biology, USA, UBE2G1 rabbit polyclonal (1:200, ABIN1385714), Bioss, USA, and Gnao1 rabbit polyclonal antibody from Aviva Systems Biology, USA.

Electrophysiology and Intrahippocampal Infusion in Anesthetized Rats

Intrahippocampal drug infusion was performed as described previously [26]. All experiments were carried out under ethical standards approved by the Norwegian Committee for Experiments on Animals. The experiments were carried out on 57 adult male rats of the Sprague-Dawley strain (Taconic, Denmark), weighing 250–350 g. Rats were anesthetized with urethane (1.5 mg/kg, i.p.), positioned in a stereotaxic frame, and body temperature was maintained at 37 °C with a thermostatically controlled electric heating pad. A concentric bipolar stimulating electrode (tip separation 500 μm; SNEX 100; Rhodes Medical Instruments, Woodland Hills, CA) was lowered into the angular bundle for stimulation of the medial perforant path. Stereotaxic coordinates for stimulation were as follows (in mm): 7.9 posterior to bregma, 4.2 lateral to the midline and 2.5 below the dura.

A Teflon-coated tungsten wire recording electrode (outer diameter of 0.075 mm; A-M Systems #7960) was glued to the infusion cannula (30 gauge). The electrode was then cut so that it extended 800 μm from the end of the cannula. Stereotaxic coordinates for recording in the dentate hilus were as follows (in mm): 3.9 posterior to bregma, 2.3 lateral and 2.8–3.1 below the dura. The recording electrode was slowly lowered into the dorsal hippocampus until a positive-going field EPSP (fEPSP) of maximum slope was obtained in the dentate hilus. The tip of the infusion cannula was located in the deep striatum lacunosum-moleculare of field CA1, 800 μm above the hilar recording site and 300–400 μm above the medial perforant synapse. The infusion cannula was connected via a polyethylene (PE50) tube to a 10-μl Hamilton syringe (Reno, NV) and infusion pump. After baseline recording for 20 min, 1 μl drug (100 μM or 1 mM in PBS, 13.5% HP transfection reagent, lot no. 139311238, Qiagen) was infused for 12 min at a rate of 0.085 μl/min. Evoked responses were recorded for 140 min after infusion. Biphasic rectangular test pulses of 150-μs duration were applied every 30 s throughout the experiment (0.033 Hz). Responses were allowed to stabilize for 1 h at a stimulation intensity that produced a population spike 30% of maximum. A stable 20-min baseline of evoked potentials was recorded (pulse-width 0.15 ms, at

0.033 Hz) before intra-hippocampal drug infusion. Evoked responses were recorded for 120 min post-infusion. Signals from the dentate hilus were amplified, filtered (0.1 Hz to 10 kHz), and digitized (25 kHz). Acquisition and analysis of field potentials were accomplished using Datawave Technologies Software. The maximum slope of the fEPSP was measured, and averages of four consecutive responses were obtained. Changes in the fEPSP slope were expressed in percent of baseline (20-min preceding infusion). Responses for input-output (I/O) curves were collected immediately before baseline recording and at 30 min and 150 min post-infusion. Seven stimulus intensities ranging from 100 to 1000 μ A were applied in randomized sequence.

Dissection of the Adult Rat Hippocampal Dentate Gyrus

After recordings were completed, the electrodes were removed, rats were decapitated and DG microdissection was carried out within 2–3 min. The brain was removed from the skull and placed onto an ice-cold glass slide where it was continuously rinsed with ice-cold PBS. The cerebellum was removed and hemispheres were separated using a scalpel along the cerebral longitudinal fissure. The hemispheres were placed dorsal side down. Forceps were used to lift the brain stem exposing the corpus callosum and the medial side of the hippocampus. The hippocampus was tilted out from the temporal cortical fold. Fimbria and blood vessels were removed. Forceps were carefully inserted into the hippocampal fissure isolating the DG from the region of Cornu Ammonis, along its septotemporal axis. The microdissected DGs were immediately frozen on dry ice and stored at -80°C until use.

Microscopy

FAM-labelled antimiR-34a and SC-miR-34a expression in hippocampal neurons was imaged on Axio Imager 2 Zeiss light fluorescent microscope.

Cell Culture and antimiR-34a Transfection

Normal rat kidney cells (NRK) were maintained in Dulbecco's modified Eagle medium (DMEM, Sigma) supplemented with 10% heat-inactivated foetal calf serum (Sigma), 100 U/ml penicillin (Sigma), 100 μ g/ml streptomycin (Sigma) and 1 mM L-glutamine at 37°C and 5% CO_2 . Cells were seeded in 12-well plates at a density of 8000 cells/ml. Hippocampal neuronal cultures were prepared with slight modifications from the protocol originally described by Banker and co-workers [27, 28]. Hippocampi of Wistar rat embryos (E18) were dissected and dissociated by trypsin treatment followed by trituration. After removal of trypsin, neurons were plated at a density of 200,000 cells/well in a 12-well

plate for biochemical analysis. Plates were precoated with poly-D-lysine (Sigma). The cultures were maintained in MEM (M2279, Sigma) growth medium supplemented with B-27 supplement (B-27® Supplement, Invitrogen), sodium bicarbonate, glucose, and pyruvate, that had been conditioned on astrocyte cultures for 3 days. Half of the neuronal growth medium was replaced with fresh growth medium twice a week. Hippocampal neurons were transfected at 8 DIV. AntimiR-34a and SC-miR-34a were transfected at a final concentration of 1 mM using HiPerFect Transfection reagent diluted to 13.5% in PBS.

The transfection mix was replaced with conditioned growth medium (neurons) or complete DMEM medium (NRK cells) after 3 h. Cells were washed with once with PBS and harvested in RNA lysis buffer (PureLink® miRNA Isolation Kit (Life technologies, Invitrogen, Carlsbad, CA, USA) after 48 h.

Cell Culture and Fluorescent-Labelled antimiR-34a

Primary hippocampal neuronal cultures were prepared from embryonic day 18 (E18) Sprague-Dawley rat brains [29, 30]. Cells were plated on coverslips coated with poly-L-lysine (100 μ g/ml) and laminin (2 μ g/ml) at a density of 30,000/well. Hippocampal cultures were grown in Minimum Essential Medium (MEM) supplemented with B27, glutamate, sodium bicarbonate, glucose, glutamate, pyruvate and antibiotic (penicillin/streptomycin/neomycin) and added to astrocyte growing plate. Fifty percent of the MEM was replaced every 3 days. Fourteen DIV neurons were incubated for 2 h with 1 μ l (1 mM) fluorescent-labelled antimiR-34a or SC-miR-34a diluted in 400-ml medium, followed by 10-min fixation by 4% paraformaldehyde/4% sucrose in PBS at room temperature. After fixation cells were washed three times in PBS for 30 min at room temperature. Slides were mounted using FluoroGold mounting medium with DAPI (Invitrogen) and image acquired on Axio imager 2 Zeiss light fluorescent microscope.

Q-PCR

To validate the inhibition of microRNAs after antimiR-34a transfection, RNA enriched in small RNAs was purified using PureLink® miRNA Isolation Kit (Life technologies, Invitrogen, Carlsbad, CA, USA). Changes in mature microRNA levels were determined using the TaqMan® MicroRNA Reverse Transcription Kit and TaqMan® microRNA Assays (Applied Biosystems, Foster City, CA) according to the manufacturer's protocol. Fifteen microliters of cDNA was generated from 30 ng of total RNA, and 3 μ l of a 15-fold dilution was used for real-time PCR reactions. The data was normalized to Y1. Changes in relative concentration were calculated with the second derivative maximum method $2^{-\Delta\text{CT}}$. ΔCT was calculated by subtracting the CT of the geometric mean of the two housekeeping genes from the CT of the gene of interest.

253 RNA Preparation

254 Micro-dissected dentate gyri were homogenized in a
 255 Dounce homogenizer on ice in lysis buffer (20 mM
 256 Tris, pH 7.5, 150 mM NaCl, 2 mM MgCl₂, 1 mM
 257 NaF, 0.5% DTT, 2 mM EDTA, protease inhibitor,
 258 RNase inhibitor, DEPC water), and protein concentra-
 259 tion was determined using the Pierce BCA protein assay
 260 reagent (Thermo Scientific, Pierce).

261 SDS-PAGE and Western Blotting

262 Equal protein amounts (40 µg) were loaded onto 8% or
 263 10% SDS-PAGE gels and run for 2 h at a constant
 264 voltage of 100 V. Separated proteins were subjected to
 265 western blotting and transferred to HyBond ECL nitro-
 266 cellulose membrane (Amersham, Little Chalfont, UK) at
 267 a constant voltage of 100 V for 1.5 h. Membranes were
 268 stained with Ponceau to check for proper transfer
 269 followed by blocking with buffer (5% BSA, 0.1%
 270 Tween and Tris-buffered saline (TBST) for 1 h on a
 271 gyro-rocker at room temperature. The primary and sec-
 272 ondary antibodies were diluted in 5% BSA in 0.1%
 273 TBST, and 0.1% TBST, respectively. The membranes
 274 were incubated with primary antibody over night at 4
 275 °C on a gyro-rocker. Following three washes of TBST,
 276 blots were incubated for 1 h in horseradish peroxidase-
 277 conjugated secondary antibody dissolved in TBST at
 278 room temperature. The blots were washed three times
 279 with TBST, and proteins were visualized using en-
 280 hanced chemiluminescence (ECL Western Blotting
 281 Analysis System, Amersham Pharmacia Biotech,
 282 Norway). The blots were scanned using Gel DOC
 283 XRS+ (BIO RAD), and densitometric analyses were
 284 performed with ImageJ software (NIH, Bethesda, MD).

285 miRNA Target Prediction

286 miRNA target prediction sources have been described
 287 elsewhere [9]. To identify the putative target genes of
 288 each miRNA, we first queried four of the most widely
 289 used target prediction sources: DIANA [31], miRanda
 290 [32], TargetScan [33] and PicTar [34]. We quantified
 291 the agreement between predicted target lists using
 292 Rank Product (RP) analysis [35]. Each gene was or-
 293 dered by quality score and the geometric mean of the
 294 gene rank calculated across prediction sources. Missing
 295 ranks were imputed for target genes missing only one
 296 rank value, and genes missing more source values were
 297 discarded. To assess the robustness of the computed
 298 ranks, we performed a bootstrap analysis with 1000
 299 permutations of rank order using the Bioconductor
 300 RankProd package [36].

Results

Given that miR-34a is implicated in the regulation of synaptic
 protein targets, it presents as an attractive candidate to manip-
 ulate for investigation of synaptic function and plasticity. In
 order to investigate the function of miR-34a the dentate gyrus
 in vivo, initial experiments were carried out in vitro for veri-
 fication of antimiR uptake in cells, cellular distribution and
 efficiency of miRNA knockdown.

AntimiR Downregulates Endogenous miRNA 34a

First, we tested endogenous knockdown of miR-34a in NRK
 cells. RNA enriched for small RNAs was isolated 48 h after
 transfection of antimiR-34a and scrambled-miR-34a (SC-
 miR-34a) control, and the level of unbound microRNA was
 assayed by RT-PCR. Approximately 8% of miR-34a remained
 unblocked after specific antimiR-34a transfection compared
 to control (Fig. 1a), demonstrating a 92% knockdown of en-
 dogenous miR-34a in vitro. Y1 RNA was used for normaliza-
 tion. Functional miRNA inhibition was also assessed in den-
 tate gyrus in vivo. Taqman qPCR was performed on dentate
 gyrus total homogenates 2 h after intrahippocampal infusion
 of SC-miR-34a or antimiR-34a (sequences listed in
 Supplementary data Table S1). Results revealed that
 antimiR-34a downregulated endogenous miR-34a 0.5-fold
 compared to SC-miR-34a control (Fig. 1b). Significance was
 tested by one-way ANOVA (**p* < 0.05). These results indicate
 that antimiR-34a is a potent inhibitor of endogenous miR-34a
 in cell cultures in vitro and in the hippocampus of live rats.

AntimiR-34a Is Detected in Cell Bodies and Dendrites of Hippocampal Neurons

To evaluate neuronal uptake, distribution and localization, an
 antimiR-34a uptake experiment was conducted using cultured
 primary hippocampal neurons. AntimiR-34a and scrambled-
 miR-34a were labelled with green fluorescent dye (FAM-6,
 Exiqon) and added (1 µl, 1 mM) to the culture medium (400
 ml) followed by an incubation period of 2 h. Fluorescence
 microscopy showed uptake of FAM-labelled antimiR-34a
 and SC-miR-34a by primary hippocampal neurons. FAM-6-
 antimiR-34a distribution was somatodendritic similar to en-
 dogenous miR34a (Fig. 2), whereas FAM labelled SC-miR-
 34a was more soma restricted. These results indicate effective
 neuronal uptake and somatodendritic distribution of antimiR-
 34a.

miRNA-34a Acutely Regulates Synaptic Efficacy

We asked whether miR-34a is involved in the regulation of
 basal synaptic efficacy in the dentate gyrus of the adult anes-
 thetized rat. AntimiR-34a and scrambled antimiR-34a were

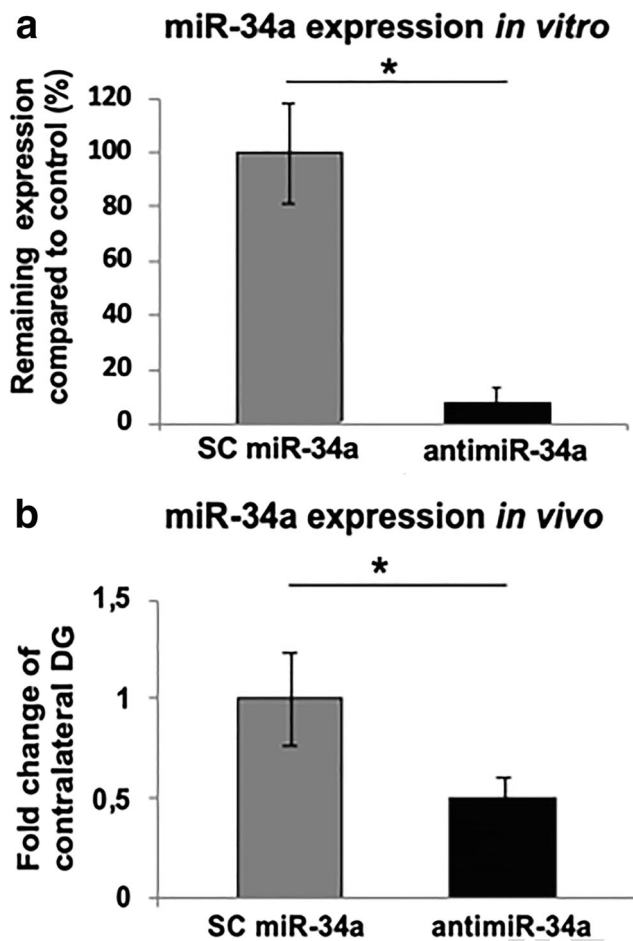


Fig. 1 AntimiR downregulates endogenous microRNA. **a** RNA enriched for small RNAs was isolated 48 h after transfection of anti-miR and scrambled control, and the level of unbound microRNAs was assayed by real-time PCR. Approximately 8% of miR-34a remained unblocked after specific anti-miR-34a transfection compared to scrambled control. Y1 was used for normalization. **b** Taqman qPCR was performed on dentate gyrus total homogenates 2 h after infusion of scrambled anti-miR-34a or anti-miR-34a. Bar graphs shows relative miRNA-34a expression levels post-anti-miR-34a ($n = 6$) and SC-anti-miR-34a ($n = 4$) treatment. Anti-miR-34a reduced endogenous miR-34a levels by 50% compared to SC-miR-34a control. Normalised to Y1 and SNO. Values are means of \pm S.E.M. One-way ANOVA analysis was used to test significance between groups ($*p < 0.05$)

during baseline (1), 30 min post-infusion (2) and 150 min after time point of infusion (3) (Fig. 3e) show a decrease in synaptic transmission across a range of stimulus intensities. Figure 3d shows representative sweeps collected at five time points before and after infusion (as labelled in Fig. 3b).

To further assess the specificity of the anti-miR-34a effect, rats were infused with mismatch-anti-miRNA-34a (MM-anti-miR-34a, striped triangles, $n = 6$) harbouring nucleotide mismatches at nucleotides 2, 6, and 10 in the 15-nt sequence (Supplementary S1). Similar to scrambled miR-34a, infusion of MM-anti-miR-34a did not impact field EPSP slope values across the duration of recording (Fig. 3b), and no difference was found between pre and post-infusion input-output curves (Fig. 3e) ($p > 0.05$). These results indicate that perfect base pair complementarity at miR-34a nucleotides 2, 6 and 10 are crucial for inhibition of endogenous miR-34a and acute downregulation of synaptic transmission. Previously, we identified Arc-targeting miRNAs and showed that overexpression of both miR-34a and miR-193 inhibits Arc expression in cultured hippocampal neurons. In adult dentate gyrus, miR-193 has a somatodendritic expression profile similar to miR-34a. However, as shown in Fig. 3a, infusion of anti-miR-193 (white circles, $n = 6$) did not elicit a change in MPP-evoked fEPSPs. The robust effect of anti-miR-34a and complete lack of effect of SC-miR-34a, MM-anti-miR-34a, and anti-miR-193 indicates a profound role of endogenous miR-34a in regulation of basal synaptic efficacy in vivo. Western blots on total homogenates showed that anti-miR-34a enhances expression of Arc 3.1-fold in the ipsilateral infused dentate gyrus relative to control (Fig. 5a, b), whereas scrambled miR-34a and mismatched anti-miR-34a controls had no significant effect ($n = 6$, $p > 0.05$).

LTP Induction Blocks Antimir-34a-Mediated Depression

Next, we sought to inhibit endogenous miR-34a during LTP in the dentate gyrus of the adult anaesthetised rat in vivo. Our previous work has shown that Arc translation is necessary for LTP consolidation [26] and that miR-34a downregulates Arc protein in vitro [5]. Given the profound depression of synaptic transmission elicited by anti-miR-34a at baseline, we wanted to assess the effect of anti-miR-34a infusion during the maintenance phase of LTP. We speculated that if miR-34a is derepressed following high-frequency stimulation (HFS)-induced LTP, the effect of anti-miR-34a infusion during the LTP maintenance phase may be attenuated. Figure 4a shows the experimental design. HFS (400 Hz, 8-pulse bursts) of the medial perforant path (MPP) generated a lasting increase in the slope of the fEPSP. Anti-miR-34a or SC-miR-34a was infused (1 μ l/12 min) at 2 h post-HFS, and recording was continued to 4 h post-HFS. Time course plots are shown in Fig 4c. Remarkably, infusion of anti-miR-34a during LTP maintenance had no effect on fEPSPs recording over the 2-h post-

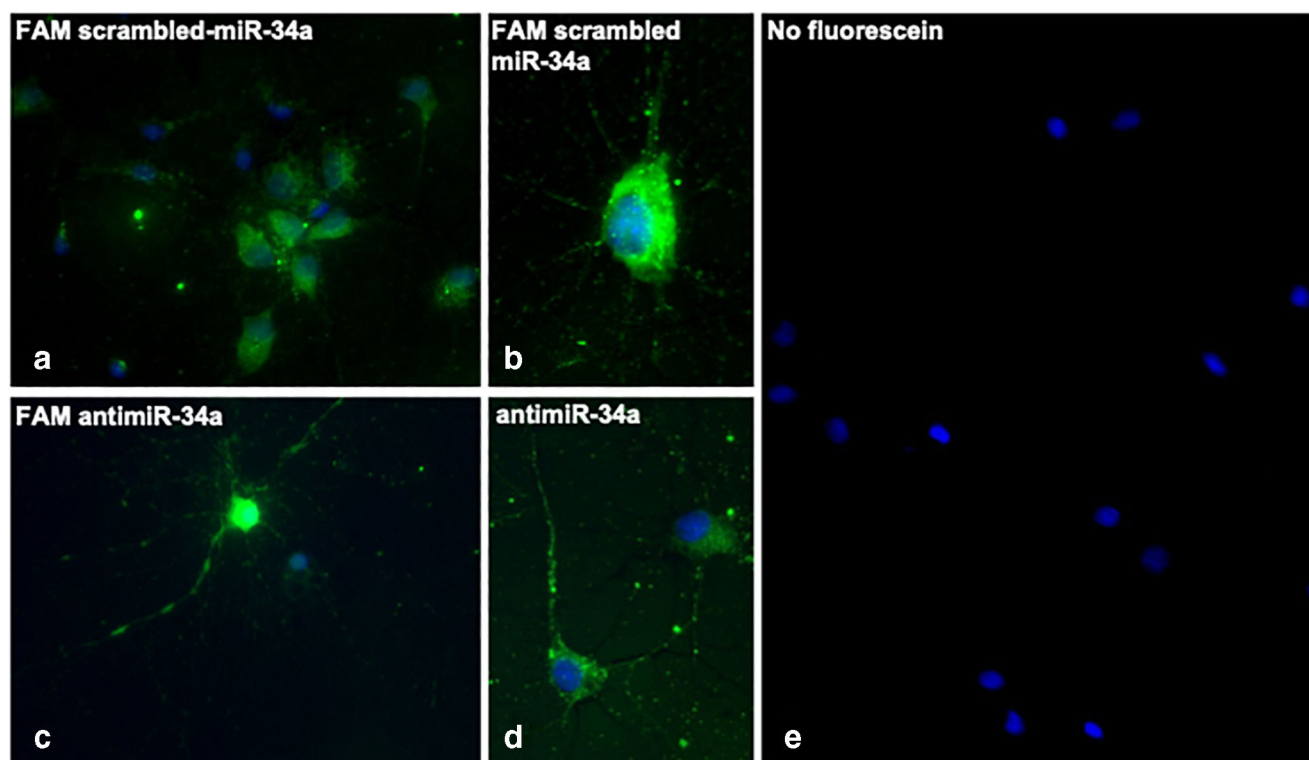


Fig. 2 AntimiR-34a is detected in cell bodies and dendrites of hippocampal neurons. Cultured hippocampal neurons (DIV 14) were treated with fluorescent anti-miR-34a or scrambled anti-miR-34a for 2 h. Expression was assessed by light microscopy. **a, b** Representative image of cells treated with fluorescent scrambled miR-34a. **c, d** Representative images of cells treated with anti-miR-34a. Anti-miR-34a is detected in the somata and the dendrites. **e** Dapi stained control, no fluorescence

infusion period, and there was no difference between anti-miR-34a and SC-miR-34a groups in LTP magnitude recorded 4 h post-HFS. Figure 4b shows representative sweeps collected at five different time points before and after HFS and drug infusion (indicated in Fig. 4c). Western blot analysis performed on whole dentate gyrus lysates confirmed upregulation of Arc protein 4 h post-HFS, but there was no significant differences in Arc levels between anti-miR-34a ($n = 5$) and SC-miR-34a ($n = 6$) infused rats (Fig. 4d). Significance was tested by one-way ANOVA ($*p < 0.05$).

mRNA Target Prediction

To better understand the downstream effects of anti-miR infusion, we integrated predictions from four miRNA target prediction resources: PicTar [34], TargetScan [33], Miranda [32] and DIANA [31]. We used the rank product method [35, 36] where ranks are aggregated across prediction resources using a geometric mean where a gene must appear in at least two sources. This allowed us to mitigate for the poor agreement normally found between different target gene prediction algorithms. miR34a was predicted to target 397 genes (Supplementary S2). Using the Bioconductor KEGG profile package, the common targets were predicted to be involved in 96 pathways (Supplementary S3), including regulation of the

actin cytoskeleton, LTD, MAPK signalling, axon guidance and the calcium signalling pathway. Five predicted targets were selected as candidates for Western blot analysis: Bcl11b/Ctip2 (from now on referred to as Ctip2), Ube2g-11, TCF4, PKI-1 α and Gnao1. Ctip2, COUP-TF interacting protein 2, is expressed predominantly in central nervous system (CNS). In the dentate gyrus, loss of Ctip2 expression selectively impairs spatial working memory [37]. TCF4 is a transcription factor known to regulate synaptic plasticity and memory function [38]. Ube2g1 is involved in mechanisms targeting abnormal or short-lived proteins for degradation [39]. PKI-1 α negatively modulates synaptic activity [40]. Gnao1 is brain-enriched and mutations in the gene are associated with epileptic encephalopathy [41].

miRNA-34a Regulates Multiple Targets in Addition to Arc in the Dentate Gyrus In vivo

Next, we investigated the effects of acute intrahippocampal infusion of anti-miR-34a on Arc protein expression along with the five new predicted miR-34a targets Ctip2, PKI-1 α , Ube2g-11, TCF4 and Gnao1 protein expression. Dentate gyri were micro-dissected 140 min after infusion of anti-miR-34a or control sequences. Replicating results from Fig. 3, anti-miR-34a infusion elicited a stable decrease of the fEPSP slope to ~

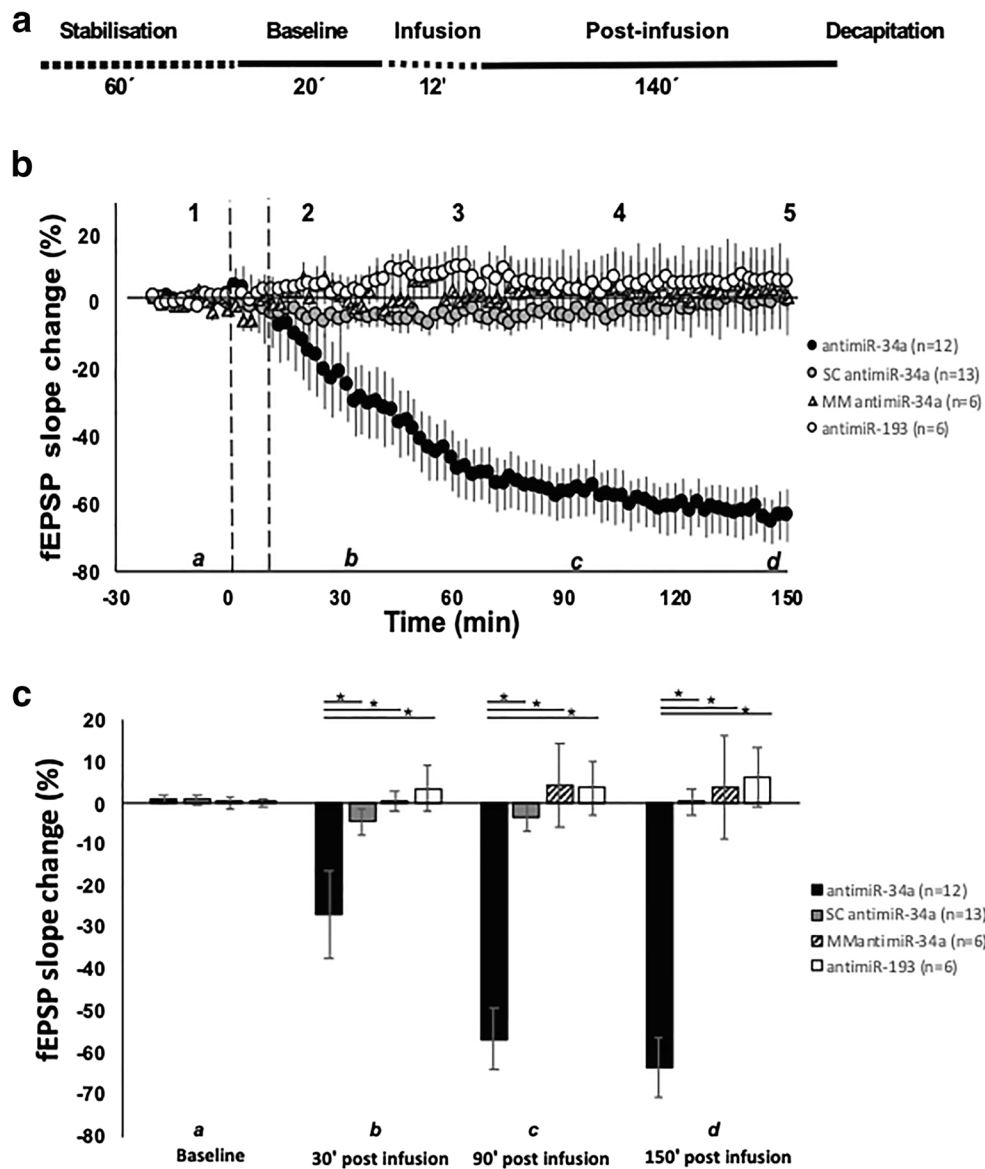


Fig. 3 miRNA-34a regulates synaptic efficacy, and variation in sequence alters target recognition. **a** Experimental design. **b** Time course plots show changes in the medial perforant path-evoked fEPSP slope expressed in percentage change from baseline. Values are means \pm S.E.M. Infusion of scrambled anti-miR-34a and anti-miR-34a is indicated by vertical, dotted lines. Synaptic efficacy is rapidly and gradually reduced to $\sim 60\%$ after local infusion (1 μ l, 1 mM) of anti-miR-34a (black circles, $n = 12$). Infusion of the multiple controls scrambled anti-miR-34a (grey circles, $n = 13$), or mismatched anti-miR-34a (striped triangles, $n = 6$) or anti-miR-193 (white circles, $n = 6$), had no effect on synaptic efficacy. **c** Bar graph of % fEPSP slope change from baseline. **d** Representative progression sweeps of scrambled anti-miR-34a, anti-miR-

34a, anti-miR-193, mismatch anti-miR-34a during baseline (1), 20 min post-infusion (2), 60 min post-infusion (3), 90 min post-infusion (4), and 120 min post-infusion (5). Averaged field potentials traces (20 sweeps) collected at the beginning of baseline recording (1), 20 min after infusion (2), 60 min post-infusion (3), 90 min post-infusion (4), and 150 min post-infusion (5). Scale bars 5 mV, 2 ms. **e** Input-output curves (average of 4 sweeps) collected at baseline (20 min), post-infusion (30 min) and at the end of the experiment (150 min). Significance was tested by factorial ANOVA, and post hoc tests. A probability level of $p < 0.05$ was considered statistically significant ($b = *p < 0.05$, $c = **p < 0.01$, and $d = ***p < 0.001$)

60% of baseline. Western blot analysis of dentate gyrus homogenates showed significantly enhanced expression of Arc (3.1-fold, $n = 6$, $p > 0.05$), Ctip2 (1.6-fold, $n = 13$, $p > 0.05$), PKI-1 α (2.2-fold, $n = 10$, $p > 0.05$), Ube2g-1 (1.5-fold, $n = 10$, $p > 0.05$) and TCF4 (2.6-fold, $n = 6$, $p > 0.05$) in the anti-miR-infused dentate gyrus relative to the contralateral dentate gyrus, which

was significantly different from the MM-anti-miR-34a and SC-miR-34a controls (Fig. 5a, b). There was no statistically significant alteration in Gnao1 expression ($n = 12$, $p < 0.05$), or difference between groups indicating that Gnao1 is not regulated by miR-34a under the present conditions. GAPDH was used as a loading control and for normalisation.

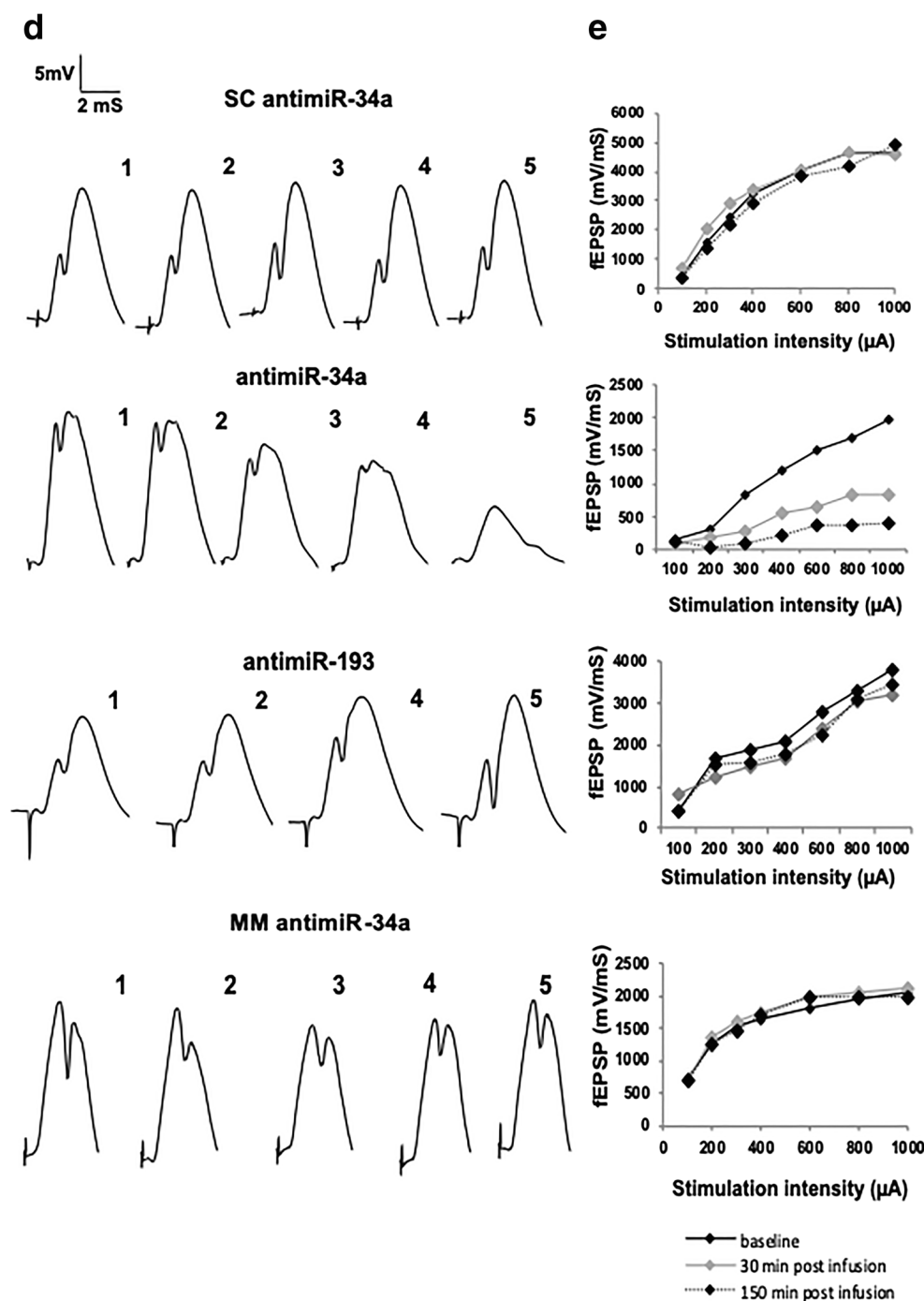


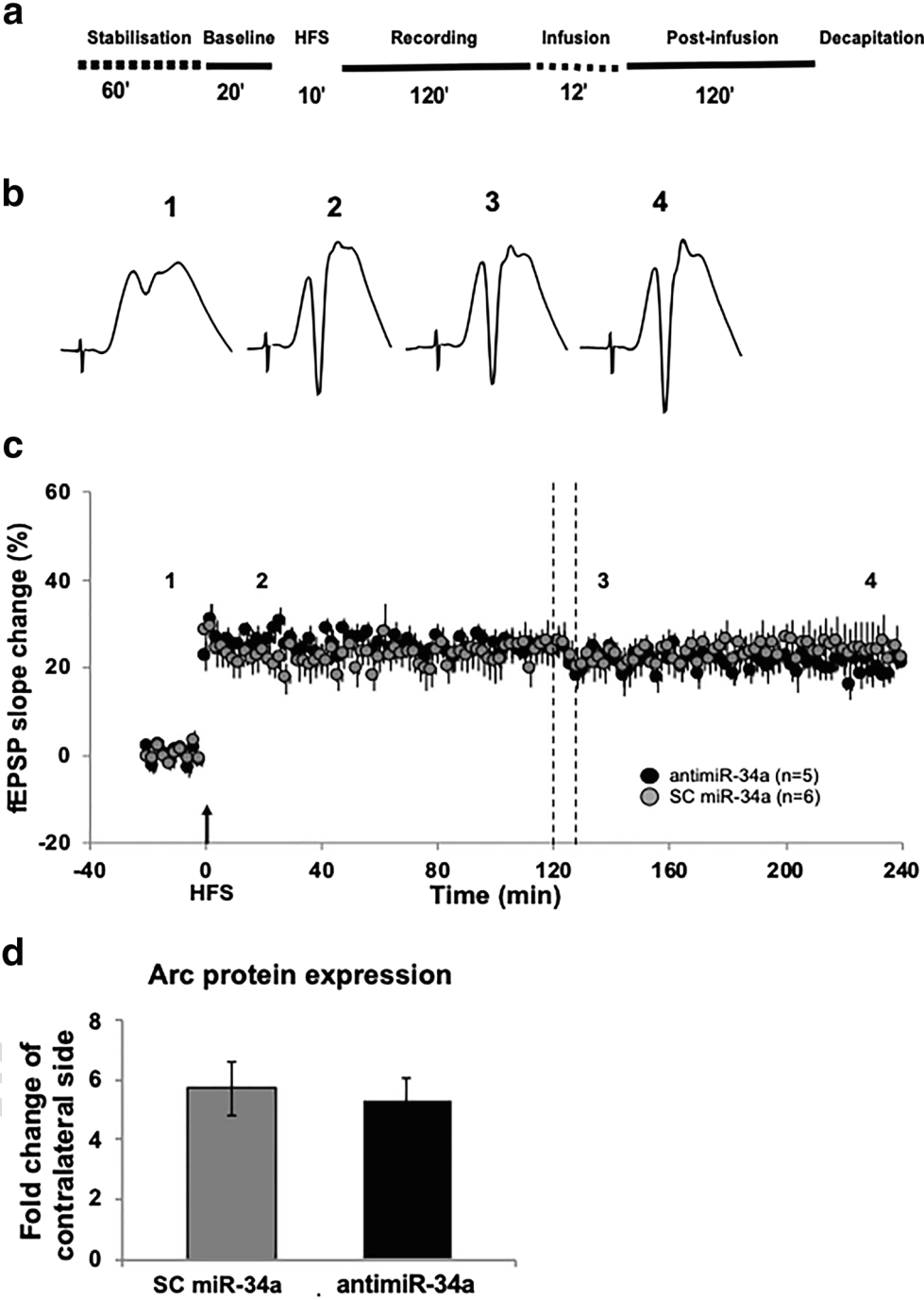
Fig. 3 (Continued)

Discussion

Synaptic plasticity such as LTP, LTD and homeostatic synaptic scaling are alterations of synaptic transmission and efficacy in response to neural activity. Long-lasting activity-dependent modifications of synapses typically require de novo protein synthesis. In addition to somatic protein synthesis, translation of mRNA in dendritic processes is important for synaptic

homeostasis and plasticity [42, 43]. Many miRNAs are involved in the spatial-temporal control of neuronal protein synthesis and regulation of synaptic plasticity. MicroRNA function has been elucidated primarily through loss-of-function approaches in which a specific miRNA is deleted or chronically inhibited, and by viral vector-mediated miRNA overexpression [7]. However, the regulation of protein synthesis during activity-dependent synaptic plasticity operates on a

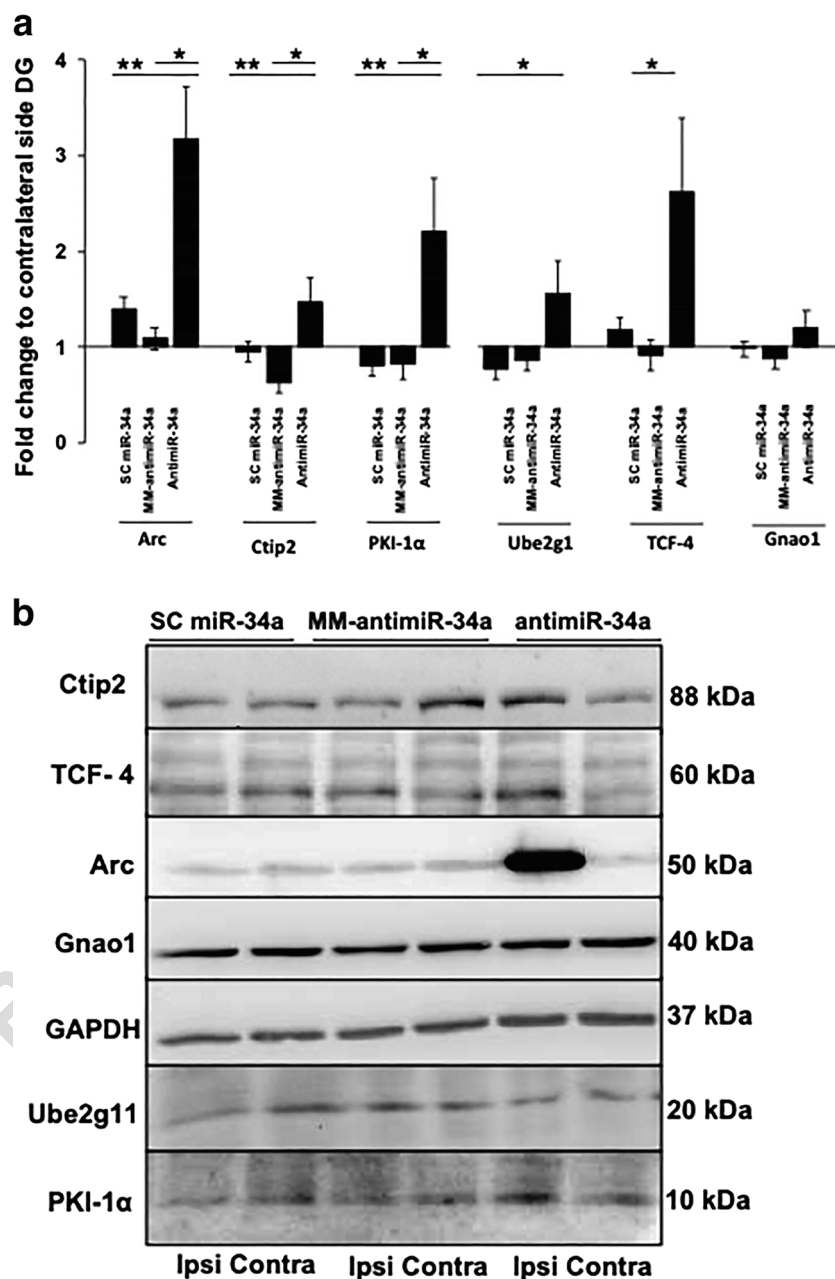
Fig. 4 LTP induction blocks miRNA-34a-mediated depression of synaptic transmission. **a** Experimental timeline. **b** Representative sweeps collected at baseline (20 min) (1), 5 min post-HFS (2), 130 min post-HFS (3) and 240 min post-HFS (4). **c** Time course plots show changes in the medial perforant path-evoked fEPSP slope expressed in percentage of baseline. Values are means \pm S.E.M. Scale bars 5 mV, 2 ms. Vertical dotted lines indicate infusion (1 μ L/12 min). HFS is indicated by black arrow (antimiR-34a, $n = 5$; SC-miR-34a, $n = 6$). Dentate gyrus tissue was collected 2 h post-infusion. **d** Western blots were performed in dentate gyrus homogenates 4 h after HFS and 2 h after infusion of antimiR-34a or SC-miR-34a during LTP. Arc protein is significantly enhanced during LTP, but there is no significant difference between the two groups ($n = 4$ in both groups)



484 timescale of minutes. To our knowledge, the present study is
485 the first to report acute regulation of synaptic efficacy in the
486 adult brain by a miRNA.
487 We found that brief (12 min) intrahippocampal infusion of
488 antimiR-34a results in a rapid and persistent decrease in
489 MMP-evoked synaptic transmission in the dentate gyrus.
490 The decrease in fEPSP started at approximately 9 min after
491 completing the infusion and developed gradually, reaching a
492 stable 60% decrease relative to pre-infusion baseline. This
493 modulation was absent when a scrambled or mismatched

miR-34a sequence was introduced. Levels of endogenous
antimiR-34a in the dentate gyrus were downregulated by
antimiR-34a, but not by infusion of scrambled control se-
quence. Furthermore, antimiR-34a but not control sequences
resulted in upregulation of Arc, a known miR-34a target and
major regulator of synaptic plasticity. AntimiR-34a infusion
similarly resulted in sequence-specific upregulation of several
novel predicted miR34a targets (Ctip2, PKI-1 α , TCF4 and
Ube2g) with roles in neuronal and synaptic function. This
suggests that endogenous miR-34a potentially regulates synaptic

Fig. 5 AntimiR-34a infusion enhances synaptic protein expression during basal conditions. Western blots were performed in dentate gyrus homogenates 2 h after infusion of scrambled anti-miR-34a, anti-miR-34a, and mismatched anti-miR-34a during baseline conditions. Immunoblots on total homogenates (left/right hemisphere ratio) showed that anti-miR-34a enhances expression of different protein. **a** Mean and standard deviation of the protein levels detected in western blotting. One-way ANOVA with Tukey's post hoc analysis was used to test significance between groups compared to control ($*p < 0.05$, $**p < 0.01$). **b** Representative blots of dentate gyrus protein expression 2 h post-infusion of scrambled anti-miR-34a, anti-miR-34a, and mismatched anti-miR-34a, relative to right hemisphere control, during baseline conditions



transmission through sequence-specific inhibition of one or more target RNAs. Release of the tonic inhibition mediated by miR-34a resulted in profound depression of synaptic transmission. Remarkably, anti-miR-34a had no effect on synaptic efficacy when infused at 2 h post-HFS, during the process of Arc-dependent LTP consolidation.

MiR-34a Regulation of Arc and Synaptic Efficacy In vivo

The speed at which anti-miR-34a impacts synaptic transmission suggests that the effective target mRNAs are located near synapses, such that newly synthesized proteins can exert a

nearly immediate effect on synaptic efficacy. Arc is a miR-34a target that may fit such a role.

The diversity of Arc function in synaptic plasticity is a truly remarkable phenomenon. Arc scales neuronal action and controls excitation and inhibition through bidirectional regulation of synaptic strength. Synaptic activity can converge to alter Arc transcription and then diverge to induce different plasticity outcomes, such as AMPA-receptor endocytosis promoting LTD or actin cytoskeletal modulation promoting LTP [26, 42, 43]. In this study, we initially chose to explore miR-34a function in vivo due to its Arc-targeting properties shown in vitro [5]. We hypothesised that knockdown of miR-34a would enhance Arc expression and alter synaptic efficacy. Here,

infusion of anti-miR-34a increased Arc expression 3-fold and acutely depressed MMP-evoked fEPSPs.

Arc is an immediate early gene with low levels of basal expression [44]. Stimulus-evoked Arc transcription may occur within minutes [45, 46], and a large fraction of the new mRNA is transported into dendrites where it accumulates in region of activated synapses, presumably to be translated locally [47]. Because Arc mRNA is subject to translation-dependent degradation, it needs to be translationally repressed in order to reach synapses on distal dendrites [48–50]. The precise dendritic spatiotemporal mechanisms regulating Arc mRNA translation and repression of translation are yet to be elucidated. However, in the CA1 region of the hippocampus, application of the metabotropic glutamate receptor agonist (S)-3,5-dihydroxyphenylglycine (DHPG) induces a transcription-independent LTD that requires translation of dendritic Arc and expression of protein within 10 min of treatment [51]. In isolated synaptoneurosome preparations, in vitro stimulation with BDNF induces Arc protein synthesis in a time range of 10–30 min [52, 53]. As mentioned, Arc translation is necessary for LTP consolidation in vivo. The process depends on the provision of newly transcribed Arc, and Panja et al. [26] showed that Arc mRNA shifts from the monosome/mRNP fraction to polysomes during LTP consolidation. Recent imaging studies from hippocampal neuronal cell cultures also suggest that, at the basal state, Arc mRNA in dendrites is held quiescent in stalled polysomes. In response to glutamate stimulation, Arc is translated in less than 1 min [54]. Given the profound effect of anti-miR-34a at the basal state, it is tempting to consider that enhanced expression of Arc and other miR-34a targets is due to activation of mRNA on stalled polysomes. Both Arc mRNA and miR-34a are found in the excitatory synaptic compartment of the dentate gyrus at the unstimulated basal state [5].

The selective modulation of basal transmission by anti-miR-34a, with no effect on established LTP, is extraordinary and the underlying mechanism is unknown. The lack of effect during the LTP state might be due to (1) inability of anti-miR-34a to access miR-34a or (2) degradation of the relevant miR-34a pool. Previously we reported that LTP induction in the dentate gyrus of urethane-anesthetized rats is associated with increased, NMDAR-dependent association of miR-34a with the Ago2/RISC [9]. Perhaps this process of miR-34a loading onto Ago2 inhibits anti-miR binding. Assuming miR-34a regulates a preexisting pool of Arc mRNA on stalled polysomes, it is possible that miR-34a is degraded or sequestered in P-bodies following HFS-induced translation. In this case, the basis for anti-miR-34a induced synaptic depression will be lost. A third possibility, so far unexplored, is that newly synthesized Arc mRNA [53] is immediately translated, thus bypassing the stage of

miR-34a binding and repression. In terms of the action of the Arc protein itself, to enhance or depress synaptic transmission, this is known to be dependent on the cell signaling context [25].

miR-34a Regulation of Novel Predicted Targets: Ctip2, TCF4, PKI1- α and Ube2g1

The bioinformatic mRNA target prediction and the in vivo evidence allows us to suggest four novel miR-34a targets. However, they are not formally identified as targets by mutation of miRNA binding sites. Here, we show that acute inhibition of miR-34a initiates acute upregulation of Arc along with four additional bioinformatically predicted targets of miR-34a: Ctip2, PKI-1 α , TCF4 and Ube2g.

Ctip2 is a C₂H₂ zinc-finger transcription factor, highly expressed in dentate granule cells. Selective ablation of Ctip2 in the adult dentate gyrus results in morphological changes leading to functional impairment [39]. Experiments in cultured striatal cell lines indicate that Ctip2 regulates a multitude of genes, and enhances brain-derived neurotrophic factor (BDNF) signalling [55] which activates cascades such as PLC/PKC, PI3K/Akt, Ras/Erk, AMPK/ACC and NF κ B pathways [56]. BDNF plays a critical role in plasticity at glutamatergic and GABAergic synapses by both pre- and postsynaptic mechanisms [57] and contributes to both acute and homeostatic alterations in hippocampal synaptic function [58]. BDNF is also known to enhance Arc expression. Thus, Ctip2 regulation could potentially impact synaptic transmission indirectly. However, the rapid decrease in synaptic transmission is less likely to involve transcription and regulation of BDNF secretion and signalling.

TCF4 is a transcription factor known to regulate synaptic plasticity and memory function [38]. TCF4 haploinsufficient mice have been studied as an animal model of autism spectrum disorder. These TCF4-deficient mice have impaired Arc expression and enhanced LTP induction in hippocampal region CA1. In our investigation of anti-miR-34a effect, expression of TCF4 and Arc protein were both enhanced while basal synaptic transmission was depressed. Though the mechanisms are unknown, the opposite effects on synaptic transmission are consistent with a homeostatic role of Arc. Interestingly, ablation of TCF4 results in downregulation Ube2g1 gene transcription, another predicted target of miR-34a [59]. Our western blots on total homogenates showed that infusion of anti-miR-34a enhances Ube2g1 expression 1.5-fold during basal conditions. However, Ube2g1 is not a dendritically located transcript [60]. This indicates that our observed increase in Ube2g1 expression may be secondary to enhanced TCF4 expression, not a result of direct miR-34a-mediated mRNA derepression. Mechanisms involving somatic translation of Ube2g1 do not present a likely explanation for the observed acute modulation of synaptic efficacy.

PKI-1 α is a member of the cAMP-dependent protein kinase (PKA) inhibitor family. PKA enhances excitatory synaptic transmission in the dentate gyrus [61], whereas PKI negatively modulates synaptic activity and regulates gene expression induced by PKA [61]. In the dentate gyrus, PKI1 α mRNA and protein is down regulated by strong depolarization [62]. However, chronic infusion of antisense oligonucleotides against PKI α into the rat brain results in a dramatic reduction of excitability and ability to exhibit LTP and LTD [62]. Here, we demonstrate that infusion of antimiR-34a during baseline conditions results in a 2.2-fold increase in PKI1 α protein expression. However, if PKI1 α is a direct mRNA target regulated by miR-34a, we would expect an effect of antimiR-34a infusion also during LTP.

Gano1 (G protein subunit alpha 1) constitutes up to 0.5% of cerebral membrane protein [63], and mutations in Gnao1 are linked to epileptic encephalopathy [41], indicating an important role in brain function. Here, western blots on total homogenates show that loss of miR-34a action does not initiate synthesis of Gano1, indicating that Gano1 is not implicated in acute regulation of synaptic transmission during baseline conditions in the dentate gyrus.

miR-34a Regulation of Synaptic Transmission in Relation to Brain Disorders

As neuroscientists, a major aim in understanding the function of miR-34a and regulation of its target genes is to contribute to new knowledge that can aid the development of novel treatment strategies for people with psychiatric and neurodegenerative brain disorders. Addressing neuropathology through antimiR strategies may be available in the near future, and the multiple benefits in using antimiR strategies have been described elsewhere [64, 65]. miR-34a targets genes that are linked to synaptic plasticity, energy metabolism and resting state network activity, and it plays a critical regulatory role in neurodegenerative diseases [15–18]. miR-34a's role in AD is far from elucidated, but there is increasing evidence of miR-34a's significance. miR-34a up- or downregulation, manipulation by overexpression or abolishment, all aid our work in understanding its memory-related mechanisms. A recent study by Sakar et al. showed that miR34-a overexpression induces rapid cognitive impairment and AD-like pathology in mice [66]. Conversely, others have shown that rats overexpressing miR-34a in the brain have better learning abilities and reduced emotionality [21]. AD model mice injected with antimiR targeting the complete miR-34 family 'rescues' memory performance [67]. In miR-34a knockout/amyloid precursor protein/presenilin 1 mice (APP/PS1), it has been confirmed that miR-34a is involved in synaptic deficits in AD pathological development, partially due to inhibition of NMDA and AMPA receptor expression [68]. Although the latter experiments are carried out in transgenic animals, they

are consistent with our observed decrease in synaptic efficacy. In sporadic AD, up-regulated miR-34a in the neocortex appears to down-regulate SHANK3, a postsynaptic scaffolding protein essential to post-synaptic structure and function [69, 70]. Others have shown that stable hippocampal miR-34a inhibition using adeno-associated virus-delivered miRNA sponges demonstrates transcriptome changes linked to neuroactive ligand-receptor transduction in cell communication, causing decreased capacity of reference memory in mice [27]. Supporting our findings, bioinformatical analyses described by Sarkar et al showed that miR-34a has the ability to affect molecular processes that are intrinsically linked to the regulation of pre- and post-synaptic neuronal excitability and resting state functional connectivity [15]. The same authors have also described that targets for miR-34a were profoundly reduced by miR-34a over-expression leading to cognitive decline and disease neuropathology [71]. Recently, it has been suggested that increasing Arc levels prior to the development of AD neuropathology could protect against cognitive impairment that accompany AD neuropathology [64]. Our results revealed that antimiR-34a infusion during basal conditions acutely depresses MMP-evoked fEPSPs due to sequence-specific mechanisms, a phenomenon that was absent during long-term potentiation. Multiple synaptic targets, including miR-34a target Arc, were upregulated during basal conditions, adding new knowledge to the complexity of miR-34a function in synaptic efficacy and plasticity. We realize that the temporal and spatial distribution of miR-34a and modulation of its targets is highly heterogeneous and serve multiple synaptic mechanistic systems and cognitive trajectories.

Conclusion

Our results identify a set of miR-34a targets associated with regulation of basal synaptic transmission in the dentate gyrus. Further work is needed to elucidate the potential causal role of these specific miR34a targets. The results described in this study are novel in the field of microRNA regulation and synaptic transmission. Current knowledge on miRNA function in synaptic plasticity and transmission in vivo is predominately based on long-term manipulations. To our knowledge, no other study has demonstrated that miRNAs are involved in acute regulation of synaptic transmission in vivo. We conclude that miRNAs can generate rapid neuronal responses and, in this way, are ideally positioned to modulate synaptic efficacy.

Funding Information This work was supported by Research Council of Norway (grants 204861 and 249951) to CB. Karin Wibrand was supported by a grant from Bergen Medical Research Foundation (BMFS). Sudarshan Patil was supported by the University of Bergen. Maciej Pajak was funded by grants EP/F500385/1 and BB/F529254/1

References

Q4 732

733
734
735
736
737
738
739
740
741
742
743
744
745
746
747
748
749
750
751
752
753
754
755
756
757
758
759
760
761
762
763
764
765
766
767
768
769
770
771
772
Q5 773
774
775
776
777
778
779
780
781
782
783
784
785
786
787
788
789
790
791
792
793
794
795

1. Filipowicz W, Bhattacharyya SN, Sonenberg N (2008) Mechanisms of post-transcriptional regulation by microRNAs: are the answers in sight? *Nat Rev Genet* 9(2):102–114
2. Kan AA, van Erp S, Derijck AA, de Wit M, Hessel EV, O'Duibhir E, de Jager W, Van Rijen PC et al (2012) Genome-wide microRNA profiling of human temporal lobe epilepsy identifies modulators of the immune response. *Cell Mol Life Sci* 69(18):3127–3145
3. Ye Y, Xu H, Su X, He X (2016) Role of MicroRNA in Governing Synaptic Plasticity. *Neural Plast* 2016:4959523
4. Earls LR, Westmoreland JJ, Zakharenko SS (2014) Non-coding RNA regulation of synaptic plasticity and memory: implications for aging. *Ageing Res Rev* 17:34–42
5. Wibrand K, Pai B, Siripommongcolchai T, Bittins M, Berentsen B, Ofte ML, Weigel A, Skaftnesmo KO et al (2012) MicroRNA regulation of the synaptic plasticity-related gene *Arc*. *PLoS One* 7(7):e41688
6. Aksoy-Aksel A, Zampa F, Schrat G (2014) MicroRNAs and synaptic plasticity—a mutual relationship. *Philos Trans R Soc Lond Ser B Biol Sci* 369(1652):20130515
7. Fu X, Shah A, Baraban JM (2016) Rapid reversal of translational silencing: emerging role of microRNA degradation pathways in neuronal plasticity. *Neurobiol Learn Mem* 133:225–232
8. Ryan B, Joilin G, Williams JM (2015) Plasticity-related microRNA and their potential contribution to the maintenance of long-term potentiation. *Front Mol Neurosci* 8:4
9. Pai B, Siripommongcolchai T, Berentsen B, Pakzad A, Vieuille C, Pallesen S, Pajak M, Simpson TI et al (2014) NMDA receptor-dependent regulation of miRNA expression and association with Argonaute during LTP in vivo. *Front Cell Neurosci* 7:285
10. Maag JL, Panja D, Sporild I, Patil S, Kaczorowski DC, Bramham CR, Dinger ME, Wibrand K (2015) Dynamic expression of long noncoding RNAs and repeat elements in synaptic plasticity. *Front Neurosci* 9:351
11. Gu QH, Yu D, Hu Z, Liu X, Yang Y, Luo Y, Zhu J, Li Z (2015) miR-26a and miR-384-5p are required for LTP maintenance and spine enlargement. *Nat Commun* 6:6789
12. Hu Z, Li Z (2017) miRNAs in synapse development and synaptic plasticity. *Curr Opin Neurobiol* 45:24–31
13. Rajgor D, Sanderson TM, Amici M, Collingridge GL, Hanley JG (2018) NMDAR-dependent Argonaute 2 phosphorylation regulates miRNA activity and dendritic spine plasticity. *EMBO J* 37(11)
14. Banerjee S, Neveu P, Kosik KS (2009) A coordinated local translational control point at the synapse involving relief from silencing and MOV10 degradation. *Neuron*. 64(6):871–884
15. Sarkar S, Jun S, Rellick S, Quintana DD, Cavendish JZ, Simpkins JW (2016) Expression of microRNA-34a in Alzheimer's disease brain targets genes linked to synaptic plasticity, energy metabolism, and resting state network activity. *Brain Res* 1646:139–151
16. Fries GR, Carvalho AF, Quevedo J (2018) The miRNome of bipolar disorder. *J Affect Disord* 233:110–116
17. Bavarian S, Mellios N, Lalonde J, Fass DM, Wang J, Sheridan SD, Madison JM, Zhou F et al (2015) Dysregulation of miR-34a links neuronal development to genetic risk factors for bipolar disorder. *Mol Psychiatry* 20(5):573–584
18. Kim AH, Reimers M, Maher B, Williamson V, McMichael O, McClay JL, van den Oord EJ, Riley BP et al (2010) MicroRNA expression profiling in the prefrontal cortex of individuals affected with schizophrenia and bipolar disorders. *Schizophr Res* 124(1–3):183–191
19. Rokavec M, Li H, Jiang L, Hermeking H (2014) The p53/miR-34 axis in development and disease. *J Mol Cell Biol* 6(3):214–230
20. Jesionek-Kupnicka D, Braun M, Trąbska-Kluch B, Czech J, Szybka M, Szymańska B, Kulczycka-Wojdala D, Bieńkowski M

- et al (2019) MiR-21, miR-34a, miR-125b, miR-181d and miR-648 levels inversely correlate with MGMT and TP53 expression in primary glioblastoma patients. *Arch Med Sci* 15(2):504–512
21. Farooqi AA, Tabassum S, Ahmad A (2017) MicroRNA-34a: a versatile regulator of myriads of targets in different cancers. *Int J Mol Sci* 18(10):E2089
22. Bommer GT, Gerin I, Feng Y, Kaczorowski AJ, Kuick R, Love RE, Zhai Y, Giordano TJ et al (2007) p53-mediated activation of miRNA34 candidate tumor-suppressor genes. *Curr Biol* 17(15):1298–1307
23. Agostini M, Tucci P, Killick R, Candi E, Sayan BS, Rivetti di Val Cervo P, Nicotera P, McKeon F et al (2011) Neuronal differentiation by Tap73 is mediated by microRNA-34a regulation of synaptic protein targets. *Proc Natl Acad Sci U S A* 108(52):21093–21098
24. Ryan MM, Ryan B, Kyrke-Smith M, Logan B, Tate WP, Abraham WC, Williams JM (2012) Temporal profiling of gene networks associated with the late phase of long-term potentiation in vivo. *PLoS One* 7(7):e40538
25. Nikolaienko O, Patil S, Eriksen MS, Bramham CR (2018) Arc protein: a flexible hub for synaptic plasticity and cognition. *Semin Cell Dev Biol* 77:33–42
26. Panja D, Kenney JW, D'Andrea L, Zalfa F, Vedeler A, Wibrand K, Fukunaga R, Bagni C et al (2014) Two-stage translational control of dentate gyrus LTP consolidation is mediated by sustained BDNF-TrkB signaling to MNK. *Cell Rep* 9(4):1430–1445
27. Malmevik J, Petri R, Knauff P, Brattås PL, Åkerblom M, Jakobsson J (2016) Distinct cognitive effects and underlying transcriptome changes upon inhibition of individual miRNAs in hippocampal neurons. *Sci Rep* 6:19879
28. Mollinari C, Racaniello M, Berry A, Pieri M, de Stefano MC, Cardinale A, Zona C, Cirulli F et al (2015) miR-34a regulates cell proliferation, morphology and function of newborn neurons resulting in improved behavioural outcomes. *Cell Death Dis* 6:e1622
29. Banker GA, Cowan WM (1977) Rat hippocampal neurons in dispersed cell culture. *Brain Res* 126(3):397–342
30. Kaech S, Banker G (2006) Culturing hippocampal neurons. *Nat Protoc* 1(5):2406–2415
31. Karagkouni D, Paraskevopoulou MD, Chatzopoulos S, Vlachos IS, Tastsoglou S, Kanellos I, Papadimitriou D, Kavakiotis I et al (2018) DIANA-TarBase v8: a decade-long collection of experimentally supported miRNA-gene interactions. *Nucleic Acids Res* 46(D1):D239–D245
32. Betel D, Wilson M, Gabow A, Marks DS, Sander C (2008) The microRNA.org resource: targets and expression. *Nucleic Acids Res*. 36:D149–53.
33. Friedman RC, Farh KK, Burge CB, Bartel DP (2009) Most mammalian mRNAs are conserved targets of microRNAs. *Genome Res* 19(1):92–105
34. Lall S, Grün D, Krek A, Chen K, Wang YL, Dewey CN, Sood P, Colombo T et al (2006) A genome-wide map of conserved microRNA targets in *C. elegans*. *Curr Biol* 16(5):460–471
35. Breitling R, Armengaud P, Amtmann A, Herzyk P (2004) Rank products: a simple, yet powerful, new method to detect differentially regulated genes in replicated microarray experiments. *FEBS Lett* 573(1–3):83–92
36. Hong F, Breitling R, McEntee CW, Wittner BS, Nemhauser JL, Chory J (2006) RankProd: a bioconductor package for detecting differentially expressed genes in meta-analysis. *Bioinformatics*. 22(22):2825–2827
37. Simon R, Baumann L, Fischer J, Seigfried FA, De Bruyckere E, Liu P, Jenkins NA, Copeland NG et al (2016) Structure-function integrity of the adult hippocampus depends on the transcription factor Bcl11b/Ctip2. *Genes Brain Behav* 15(4):405–419
38. Kennedy AJ, Rahn EJ, Paulukaitis BS, Savell KE, Kordasiewicz HB, Wang J, Lewis JW, Posey J et al (2016) TCF4 Regulates

- 862 Synaptic Plasticity, DNA Methylation, and Memory Function. *Cell*
863 Rep 16(10):2666–2685
- 864 39. Stewart MD, Ritterhoff T, Klevit RE, Brzovic PS (2016) E2 en-
865 zymes: more than just middle men. *Cell Res* 26(4):423–440
- 866 40. Dalton GD, Dewey WL (2006) Protein kinase inhibitor peptide
867 (PKI): a family of endogenous neuropeptides that modulate neuro-
868 nal cAMP-dependent protein kinase function. *Neuropeptides*.
869 40(1):23–34
- 870 41. Nakamura K, Kodera H, Akita T, Shiina M, Kato M, Hoshino H,
871 Terashima H, Osaka H et al (2013) De Novo mutations in GNAO1,
872 encoding a G α subunit of heterotrimeric G proteins, cause epilep-
873 tic encephalopathy. *Am J Hum Genet* 93(3):496–505
- 874 42. Bramham CR, Wells DG (2007) Dendritic mRNA: transport, trans-
875 lation and function. *Nat Rev Neurosci* 8(10):776–789
- 876 43. Tom Dieck S, Hanus C, Schuman EM (2014) SnapShot: local pro-
877 tein translation in dendrites. *Neuron*. 81(4):958–958
- 878 44. Carmichael RE, Henley JM (2018) Transcriptional and post-
879 translational regulation of Arc in synaptic plasticity. *Semin Cell*
880 Dev Biol 77:3–9
- 881 45. DaSilva LL, Wall MJ, P de Almeida L, Wauters SC, Januário YC,
882 Müller J, Corrêa SA (2016) Activity-Regulated Cytoskeleton-
883 Associated Protein Controls AMPAR Endocytosis through a
884 Direct Interaction with Clathrin-Adaptor Protein 2. *eNeuro* 3(3):
885 ENEURO.0144-15.2016
- 886 46. Rao VR, Pintchovski SA, Chin J, Peebles CL, Mitra S, Finkbeiner S
887 (2006) AMPA receptors regulate transcription of the plasticity-
888 related immediate-early gene Arc. *Nat Neurosci* 9(7):887–895
- 889 47. Guzowski JF, McNaughton BL, Barnes CA, Worley PF (1999)
890 Environment-specific expression of the immediate-early gene
891 Arc in hippocampal neuronal ensembles. *Nat Neurosci* 2(12):
892 1120–1124
- 893 48. Ramírez-Amaya V, Vazdarjanova A, Mikhael D, Rosi S, Worley
894 PF, Barnes CA (2005) Spatial exploration-induced Arc mRNA and
895 protein expression: evidence for selective, network-specific reactivation.
896 *J Neurosci* 25(7):1761–1768
- 897 49. Farris S, Lewandowski G, Cox CD, Steward O (2014) Selective
898 localization of arc mRNA in dendrites involves activity- and
899 translation-dependent mRNA degradation. *J Neurosci* 34(13):
900 4481–4493
- 901 50. Steward O, Farris S, Pirbhoy PS, Darnell J, Driesche SJ (2015)
902 Localization and local translation of Arc/Arg3.1 mRNA at synap-
903 ses: some observations and paradoxes. *Front Mol Neurosci* 7:101
- 904 51. Waung MW, Pfeiffer BE, Nosyreva ED, Ronesi JA, Huber KM
905 (2008) Rapid translation of Arc/Arg3.1 selectively mediates
906 mGluR-dependent LTD through persistent increases in AMPAR
907 endocytosis rate. *Neuron*. 59(1):84–97
- 908 52. Yin Y, Edelman GM, Vanderklish PW (2002) The brain-derived
909 neurotrophic factor enhances synthesis of Arc in
910 synaptoneurosomes. *Proc Natl Acad Sci U S A* 99(4):2368–2373
- 911 53. Messaoudi E, Kanhema T, Soulé J, Tiron A, Dayte G, da Silva B,
912 Bramham CR (2007) Sustained Arc/Arg3.1 synthesis controls
913 long-term potentiation consolidation through regulation of local
914 actin polymerization in the dentate gyrus in vivo. *J Neurosci*
915 27(39):10445–10455
- 916 54. Na Y, Park S, Lee C, Kim DK, Park JM, Sockanathan S, Haganir
917 RL, Worley PF (2016) Real-Time Imaging Reveals Properties of
918 Glutamate-Induced Arc/Arg 3.1 Translation in Neuronal Dendrites.
919 *Neuron*. 91(3):561–573
- 920 55. Joilin G, Guévremont D, Ryan B, Claudianos C, Cristino AS,
921 Abraham WC, Williams JM (2014) Rapid regulation of
922 microRNA following induction of long-term potentiation in vivo.
923 *Front Mol Neurosci* 7:98
- 924 56. Tang B, Di Lena P, Schaffer L, Head SR, Baldi P, Thomas EA
925 (2011) Genome-wide identification of Bcl11b gene targets reveals
926 role in brain-derived neurotrophic factor signaling. *PLoS One* 6(9):
927 e23691
- 928 57. Sasi M, Vignoli B, Canossa M, Blum R (2017) Neurobiology of
929 local and intercellular BDNF signaling. *Pflugers Arch* 469(5-6):
930 593–610
- 931 58. Fortin DA, Srivastava T, Dwarakanath D, Pierre P, Nygaard S,
932 Derkach VA, Soderling TR (2012) Brain-derived neurotrophic fac-
933 tor activation of CaM-kinase kinase via transient receptor potential
934 canonical channels induces the translation and synaptic incorpora-
935 tion of GluA1-containing calcium-permeable AMPA receptors. *J*
936 Neurosci 32(24):8127–8137
- 937 59. Hammond E, Lang J, Maeda Y, Pleasure D, Angus-Hill M, Xu J,
938 Horiuchi M, Deng W et al (2015) The Wnt effector transcription
939 factor 7-like 2 positively regulates oligodendrocyte differentiation
940 in a manner independent of Wnt/ β -catenin signaling. *J Neurosci*
941 35(12):5007–5022
- 942 60. Cajigas LJ, Tushev G, Will TJ, tom Dieck S, Fuerst N, Schuman EM
943 (2012) The local transcriptome in the synaptic neuropil revealed
944 by deep sequencing and high-resolution imaging. *Neuron*.
945 74(3):453–466
- 946 61. Chen HX, Roper SN (2003) PKA and PKC enhance excitatory
947 synaptic transmission in human dentate gyrus. *J Neurophysiol*
948 89(5):2482–2488
- 949 62. de Lecea L, Criado JR, Rivera S, Wen W, Soriano E, Henriksen SJ,
950 Taylor SS, Gall CM et al (1998) Endogenous protein kinase A
951 inhibitor (PKI α) modulates synaptic activity. *J Neurosci Res*
952 53(3):269–278
- 953 63. Huff RM, Axton JM, Neer EJ (1985) Physical and westernlogical
954 characterization of a guanine nucleotide-binding protein purified
955 from bovine cerebral cortex. *J Biol Chem* 260(19):10864–10871
- 956 64. Lesuis SL, Hoeijmakers L, Korosi A, de Rooij SR, Swaab DF,
957 Kessels HW, Lucassen PJ, Krugers HJ (2018) Vulnerability and
958 resilience to Alzheimer's disease: early life conditions modulate
959 neuropathology and determine cognitive reserve. *Alzheimers Res*
960 Ther 10(1):95
- 961 65. Jaber VR, Zhao Y, Sharfman NM, Li W, Lukiw WJ (2019)
962 Addressing Alzheimer's Disease (AD) Neuropathology Using
963 Anti-microRNA (AM) Strategies. *Mol Neurobiol*
- 964 66. Sarkar S, Engler-Chiurazzi EB, Cavendish JZ, Povroznik JM,
965 Russell AE, Quintana DD, Mathers PH, Simpkins JW (2019)
966 Over-expression of miR-34a Induces Rapid Cognitive Impairment
967 and Alzheimer's Disease-like Pathology. *Brain Res* 8:146327
- 968 67. Zovoilis A, Agbemenyah HY, Agis-Balboa RC, Stilling RM,
969 Edbauer D, Rao P, Farinelli L, Delalle I et al (2011) microRNA-
970 34c is a novel target to treat dementias. *EMBO J* 30(20):4299–4308
- 971 68. Xu Y, Chen P, Wang X, Yao J, Zhuang S (2018) miR-34a deficiency
972 in APP/PS1 mice promotes cognitive function by increasing syn-
973 aptic plasticity via AMPA and NMDA receptors. *Neurosci Lett*
974 670:94–104
- 975 69. Kursula P (2019) Shanks - multidomain molecular scaffolds of the
976 postsynaptic density. *Curr Opin Struct Biol* 54:122–128
- 977 70. Zhao Y, Jaber VR, LeBeauf A, Sharfman NM, Lukiw WJ (2019)
978 microRNA-34a (miRNA-34a) mediated down-regulation of the
979 post-synaptic cytoskeletal element SHANK3 in sporadic
980 Alzheimer's disease (AD). *Front Neurol* 10:28
- 981 71. Zhao Y, Jaber V, Lukiw WJ (2016) Over-expressed pathogenic
982 miRNAs in Alzheimer's disease (AD) and prion disease (PrD) drive
983 deficits in TREM2-mediated A β 42 peptide clearance. *Front Aging*
984 Neurosci 8:140

AUTHOR QUERIES

AUTHOR PLEASE ANSWER ALL QUERIES.

- Q1. Please check if the following ORCID information's are correct.
- Q2. "13.5%" before the sentence "The transfection mix was replaced with conditioned growth medium (neurons) or complete..." was deleted. Please check if action taken is correct.
- Q3. Figures 3 and 5 contains poor quality of text in image. Otherwise, please provide replacement figure file.
- Q4. References 65 and 72 based on original manuscript we received were identical. Hence, the latter was deleted and reference list and citations were adjusted. Please check if appropriate.
- Q5. Please provide complete bibliographic details of reference [13, 65].

UNCORRECTED PROOF